Performance Evaluation of Two System Models for a MIMO System to Hover the Bicopter Unmanned Aerial Vehicle

Jalu Ahmad Prakosa[1*], Swivano Agmal[2], Edi Kurniawan[1], Muhammad Jauhar Kholili[2], and Chifayah Astuti[3]

[1]*Research Center for Photonics, National Research and Innovation Agency (BRIN) of Indonesia*
Kawasan PUSPIPTEK Building 420, South Tangerang City, 15314, Indonesia

[2]*Research Center for Quantum Physics, National Research and Innovation Agency (BRIN) of Indonesia*
Kawasan PUSPIPTEK Building 420, South Tangerang City, 15314, Indonesia

[3]*Faculty of Engineering, University of Borobudur*
Jl. Raya Kalimalang No. 1, Building C, Jakarta, 13620, Indonesia

[*]*Corresponding author. Email: jalu.ahmad.prakosa@brin.go.id*

Abstract— Building unmanned aerial vehicle (UAV) control system models are highly challenging due to multiple inputs and multiple outputs (MIMO). Not only does it have various angular position outputs such as roll, yaw, and pitch, but also flight control has more than one input; for instance, a bicopter has dual rotors. More rotors have more complex model. The hover condition has a zero resultant force which can be utilized to design a system model. On the other hand, an attractive identification system method is applied to develop the design. This research aims to evaluate the performance of two MIMO design on bicopter between methods based on the hover principle and identification technique. Experimental validation by employing bicopter simulator is an excellent strategy to fulfil this purpose. The results of the investigation of the experiment showed that the identification model was more accurate than the hover design, particularly regarding the overshot phenomenon and error. In addition, the hover principle tended to build ideal model because it did not include the dynamic, uncertainty and nonlinear conditions in aeroplane control design. Although the identification system was complicated because it previously needed to measure the input and output values, it performed closer to the actual experiment. It performed more satisfactory overshoot values compared with the experimental validation than the hover model by 1°, 3°, and 8° in roll, pitch, and yaw angles, respectively.

Keywords— bicopter; comparison; flight control; hover; MIMO model; system identification

I. INTRODUCTION

Planning in saving the budget can be applied to a design. Moreover, optimization can be used to an appropriate model design [1]. Accurate design plays an essential role in the development of control systems knowledge. The system model describes the nature of a plant's control system, which is generally described in mathematical equations, either transfer function or state-space, so it is beneficial to be developed with optimization. The improvement of control theory can be implemented on a model from robust in [2], [3] to the adaptive paradigm in [4], [5], particularly for optimization purposes.

Challenging system model can be found in airplane control because it has multiple inputs and outputs [6]. The controlled output of the flight plant is the direction of the rotating angle with three angles: roll, yaw, and pitch. The input signal to generate lift for flight is called thrust. Study in [7] described that the faster propeller rotation will increase the thrust lift. The number of rotors to generate thrust is generally more than one. For example, a bicopter in [8], [9] has two rotors of motor that are controlled to fly properly [10]. Therefore, designing a dual motor system model is exciting research with a high difficulty related to the multiple inputs and outputs [11].

Bicopter is the chosen plant model because it is a helicopter sample with many rotors that can take off more freely [9]. Each rotor comprises a direct current motor that provides dynamic, uncertainty, and nonlinear effects to the system [12], [13]. In addition, bicopters are often used as drone applications in [14]–[16]. This plant offers studies related to MIMO model design in flight control. Furthermore, this type of UAV controls dual motors, for instance, in [17], to hover in a stable position. The principle of equilibrium in the hover position is an inspiration in flight control design methods [18]. In addition, the resultant force is assumed to be zero because the downward gravitational force is equal to the upward thrust that makes the bicopter float. For this reason, it is fascinating to study the observation of the design of the bicopter system model employing the hover law. On the other hand, the previous flow rate control study in [19] showed that the identification system offers a model design approach that is no less impressive. But this method firstly requires measured data from both input and output values from a plant. Practicing both techniques, the 3 Degree of Freedom (DOF) helicopter facility, which is performed in [20], provides convenience in designing the bicopter flight system model. Because of these reasons, the difficulty of MIMO model design and performance comparison between derived model from hover principal technique and system identification method make gap in this research. This study purposed to analyze the performance of two MIMO models on the bicopter between the technique from the hover principle and the identification method. Not only graphical analysis but also accuracy comparison will be investigated between both ways to evaluate

Received 22 March 2022, Accepted 30 October 2022, Published 10 November 2022.
DOI: https://doi.org/10.15294/jte.v14i1.35746

their performances. The reviewed overshoot should determine the most suitable model. We explain our main contributions to emphasize the novelty of our research outcome and to fill our exciting gap are as follows:

- Demonstrate MIMO control system of the bicopter model from the hover circumstance technique.
- Perform system identification method to build MIMO control system for the bicopter model.
- Validate and evaluate the performance of both control system models by using experimental tools of 3 DOF helicopters as the bicopter simulator.
- Assess the accuracy through each error and overshoot between the hovering model and identification method.

II. METHOD

A. Control System Model

The control system model illustrates the trait of a plant's control system, which is commonly indicated in mathematical equations, therefore model can be improved by optimization. It also can be mentioned as dynamic system model because the control system of bicopter UAV includes dynamics of many systems, such as mechanical and electrical traits. The mathematical model of control systems design for observation is usually employed a state space model in [21], which apply state variables to describe a system by a set of first-order differential in (1) and Figure 1.

$$\dot{x} = Ax + Bu; y = Cx + Du \quad (1)$$

where x is state vector, y is output vector, u is input vector, A is state matrix, B is input matrix, C is output matrix, and D is feedforward matrix.

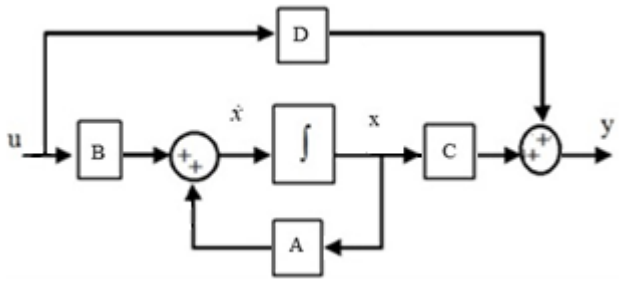

Figure 1. State-space model

Control system design for analysis in a mathematical model is also generally applied as a transfer function, the output ratio to the input of a system in the Laplace domain, which illustrates in Figure 1 and (2).

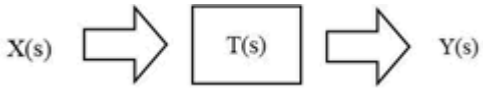

Figure 2. Transfer function block diagram

$$T(s) = \frac{Y(s)}{X(s)} \quad (2)$$

The information of variables where X(s) is input signal, T(s) is transfer function, Y(s) is output signal, and s is complex frequency.

Transfer function or state space can be obtained from the system identification procedure in [22], which uses statistical methods to build mathematical models of dynamical systems from the relation between both input and output measured data. This research is exciting because it wants to compare the performance of the control system model of bicopter between the hovering model as a white-box approach and the identification model as a black-box design [23]. The experimental setup will be explained in the appendix.

B. Derived Model from Hover Principal Method

The angles of rotation of 3 DOF helicopter is analogous with Chinook bicopter description in [9]; therefore, the pitch, roll and yaw can be shown in Figure 3 as general aircraft flight control.

Figure 3. Angles of rotation of bicoper

The set of the angle's rotation for flight control of Chinook's bicopter in Figure 3 is implemented to the 3 DOF helicopter facilities, for example, in [20], and its free body diagram is illustrated in Figure 4. The speed control from dual DC motors generates thrust force [24]. Not only the angles of rotation but also the force illustration is described in Figure 4. The signs of each axis for angles of rotation are determined.

- The horizontal position of a helicopter if r(t)=0, then roll angle becomes positive, (t)>0, a helicopter flies higher than counterweight.
- The yaw angle is positive, ɣ(t)>0, if it rotates counter-clockwise (CCW) direction.
- The angle of pitch intensify positively, p(t)>0, when the front motor is higher than the back motor.

The Newton law I work when the helicopter hovers stationary or moves at a steady speed in Figure 5. Because of that reason, the whole force sum on the free body diagram of a helicopter is zero when it hovers, which shows in (3).

$$\Delta F = F_T - W = 0 \quad (3)$$

The total torque is also zero. These circumstances apply the force equilibrium and explain the formula arriving at the system output in (4)-(7).

$$\Delta\tau = \tau_T - \tau_W = 0 \quad (4)$$

$$2.V_o.L_a.K_f = (L_w.m_w - L_a.m_f - L_a.m_b).g \quad (5)$$

$$V_o = \frac{(L_w.m_w - L_a.m_f - L_a.m_b).g}{2..L_a.K_f} \quad (6)$$

$$\begin{bmatrix} V_F \\ V_B \end{bmatrix} = K_g + \begin{bmatrix} V_o \\ V_o \end{bmatrix} \quad (7)$$

The explanation of equations (3)-(7) above can be explained as follows, where r(t), p(t), and (t) are roll angle (°), pitch angle (°), and yaw angle (°). F_T and T are force (N) and torque (N.m). W and τ_T are weight (N) and torque (N.m) because of gravity. m_w, m_f, and m_b are mass for counterweight (kg), front motor (kg), and back motor (kg). L_w and L_a are the distance between the yaw axis and helicopter body (m), and counterweight (m). L_h is the distance between the pitch axis and each motor (m). K_f is motor force-thrust constant (N/V), then V_o is quiescent voltage for motor (V). Kg is a constant gain of the close loop system (V).

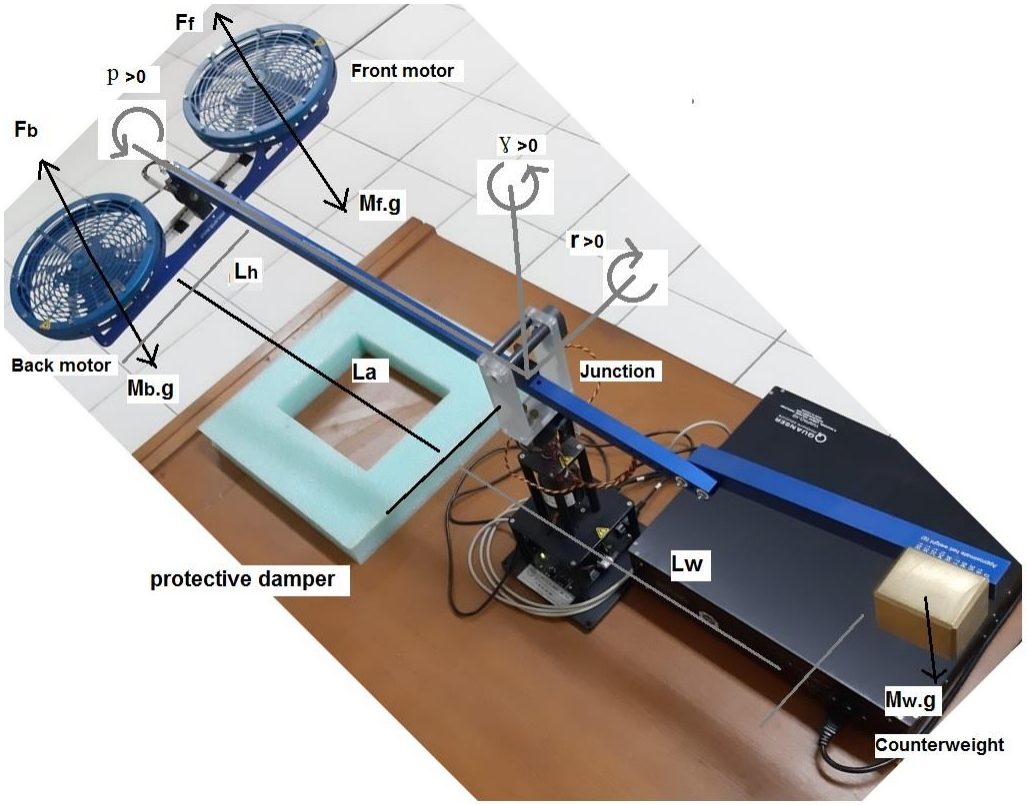

Figure 4. Free body diagram of 3 DOF helicopter

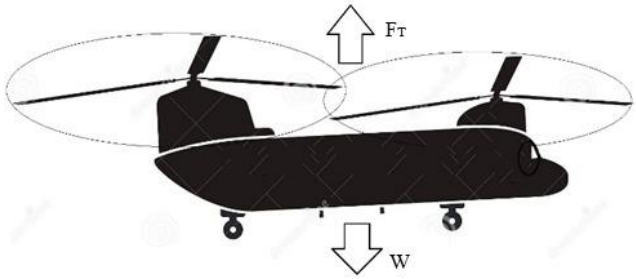

Figure 5. Hover circumstance

The state-space representation of the close loop system in Figure 1 and (1), for example, in [25], and (8) was developed from the hover equation in (7).

$$x^T = \begin{bmatrix} r & p & \gamma & \dot{r} & \dot{p} & \dot{\gamma} \end{bmatrix} \tag{8}$$

on the other hand, the output vector could be written to (9).

$$y^T = \begin{bmatrix} r & p & \gamma \end{bmatrix} \tag{9}$$

Furthermore, the other state-space matrices were set as (10)-(13), which referred to the hover principle, and then the gains for voltage output are described in (14).

$$A = \begin{bmatrix} 0 & 0 & 0 & 1 & 0 & 0 \\ 0 & 0 & 0 & 0 & 1 & 0 \\ 0 & 0 & 0 & 0 & 0 & 1 \\ 0 & 0 & 0 & 0 & 0 & 0 \\ 0 & 0 & 0 & 0 & 0 & 0 \\ 0 & \dfrac{(L_w.m_w - L_a.m_f - L_a.m_b).g}{m_w.L_w^{\,2} + 2.m_f.L_h^{\,2} + 2.m_f.L_a^{\,2}} & 0 & 0 & 0 & 0 \end{bmatrix} \tag{10}$$

$$B = \begin{bmatrix} 0 & 0 \\ 0 & 0 \\ 0 & 0 \\ \dfrac{L_a.K_f}{m_w.L_w^{\,2} + 2.m_f.L_a^{\,2}} & \dfrac{L_a.K_f}{m_w.L_w^{\,2} + 2.m_f.L_a^{\,2}} \\ \dfrac{K_f}{2.m_f.L_h^{\,2}} & -\dfrac{K_f}{2.m_f.L_h^{\,2}} \\ 0 & 0 \end{bmatrix} \tag{11}$$

$$C = \begin{bmatrix} 1 & 0 & 0 & 0 & 0 & 0 \\ 0 & 1 & 0 & 0 & 0 & 0 \\ 0 & 0 & 1 & 0 & 0 & 0 \end{bmatrix} \tag{12}$$

$$D = \begin{bmatrix} 0 & 0 \\ 0 & 0 \\ 0 & 0 \end{bmatrix} \tag{13}$$

$$K_g = \begin{bmatrix} 37.6 & 13.2 & -11.5 & 20.9 & 4.7 & -16.1 & 10.0 & -1.0 \\ 37.6 & -13.2 & 11.5 & 20.9 & -4.7 & 16.1 & 10.0 & 1.0 \end{bmatrix} \tag{14}$$

C. System Identification Method

The system identification method provides the optimal design of experiments for an efficient model, which is developed for flow rate control system in [19]. The statistical approach of the system identification, which is applied in [26], estimates the model by minimizing the error between the model output, $Y_{mod,}$ and the measured experimental results, Y_{meas}. This technique develops the identification model in (15).

$$Y_{mod}(t) = T.u(t) \quad (15)$$

System identification techniques employ both input and output of experimental data. Moreover, it designs by describing data divergence under conditions hypothesized to reflect the variation. Therefore, the distiction between the output model and the measured results or error, e, becomes minimal as possible using statistical calculations in (16) by Matlab software of System Identification Toolbox [22].

$$e(t) = Y_{meas}(t) - Y_{mod}(t) \rightarrow 0 \quad (16)$$

The system identification method may be utilized as validation way in [27]. The single input and single output (SISO) for bicopter model have been performed in [28], so the MIMO model is challenging to be conducted in this study. Furthermore, the three outputs of angle rotation, namely roll, pitch, and yaw, are obtained from the encoder sensor. On the other hand, the amplifier indicates both rotors input voltage from the front and back motors. Therefore those are employed to build the MIMO identification technique as in Figure 6. Then, the variable values of bicopter properties were described in Table I.

Error and overshoot will be applied to evaluate the performance of two comparative MIMO models. Error is the difference between measured and set values. On the other hand, overshoot is the largest difference value between the measured and set value in the step response.

TABEL I. NOMENCLATURE DESCRIPTION

No	Parameter	Unit
1	The transfer function of the system, T	-
2	Roll angle, r	°
3	Pitch angle, p	°
4	Yaw angle, ɣ	°
5	Error, e	°
6	Gravitation acceleration, g	9.81 m/s2
7	Force, F_T	N
8	Torque, τ_T	N.m
9	Weight, W	N
10	Torque because of gravitation, τ_T	N.m
11	Counterweight mass, m_w	1.87 kg
12	Front motor mass, m_f	0.575 kg
13	Back motor mass, m_b	0.575 kg
14	Distance between yaw axis and helicopter body, L_w	0.4699 m
15	Distance between yaw axis and counterweight, L_a	0.6604 m
16	Distance between pitch axis and each motor, L_h	0.1778 m
17	Motor force-thrust constant, K_f	0.1188 N/Volt
18	Gain constant, Kg	Volt
19	Quiescent voltage for motor, V_o	Volt
20	State vector, x	-
21	State matrix, A	-
22	Input matrix, B	-
23	Output matrix, C	-
24	Feedforward matrix, D	-
25	Time, t	Second (s)
26	Input signal, X	-
27	Output signal, Y	-
28	Complex frequency, s	-
29	Front motor voltage, V_F	Volt
30	Back motor voltage, V_B	Volt
31	Output model, Y_{mod}	-
32	Measured results, Y_{meas}	-

Figure 6. The block diagram for MIMO flight controller of bicopter from experiment data by system identification method

III. RESULTS AND DISCUSSION

Besides the hover model in (7) on the state-space model above, the system identification toolbox was used to develop controller design as a transfer function from actual bicopter plant behaviour data. The input data of voltage signals for both motor and the roll angle output were inserted by system identification procedure in the time domain, which accurate time is crucial in [29], as in (2) and Figure 2. The following is an identification model in the form of a MIMO transfer function:

$$T(s)_{1,1} = \frac{52s^3 + 6.568s^2 + 7.539s + 3.989}{s^4 + 1.379s^3 + 2.01s^2 + 1.072s + 0.3533}$$

$$T(s)_{1,2} = \frac{0.2395s^3 - 0.827s^2 + 1.139s}{s^4 + 1.379s^3 + 2.01s^2 + 1.072s + 0.3533}$$

$$T(s)_{1,3} = \frac{-2.821s^3 + 0.3479s^2 + 1.807s}{s^4 + 1.379s^3 + 2.01s^2 + 1.072s + 0.3533}$$

$$T(s)_{2,1} = \frac{-2.537s^3 - 6.706s^2 - 8.267s - 3.854}{s^4 + 1.379s^3 + 2.01s^2 + 1.072s + 0.3533}$$

$$T(s)_{2,2} = \frac{-0.6011s^3 + 0.5048s^2 - 1.381s - 0.314}{s^4 + 1.379s^3 + 2.01s^2 + 1.072s + 0.3533}$$

$$T(s)_{2,3} = \frac{2.19s^3 - 0.3158s^2 - 1.801s - 1.047}{s^4 + 1.379s^3 + 2.01s^2 + 1.072s + 0.3533} \quad (17)$$

The comparison of both models, which were the state space of the hover model in (8)-(14) and the transfer function of the identification model in (17), and experimental validation for roll angle control in the selected point of 10° was illustrated in Figure 7. The identification model had a more similar signal of roll angle with the experiment than the hover model, particularly on the overshoot signal. The accuracy of the control method could be investigated by overshoot and error values, which are performed in [10]. The excellent control technique would achieve the minimum overshoot and error values because they were the traits of the control system. The experimental overshoot value at the roll angle was around 23°, which was slightly different from the identification model with about 22°. On the other hand, the hover model had a much different overshoot, around 12° for the roll angle. It showed that Apart from the roll angle as the primary part of the bicopter's take-off position, two other angles, such as pitch and yaw, needed to be investigated between both models because

the MIMO model had various outputs, as many as three-angle rotations in this case.

Although the two models were not similar to the experimental results on the pitch angle in Figure 8, the results of the identification system provided better validation, especially the error is close to 3°. Moreover, the signal value of the hover model was excessively ideal to have zero error. The outcome of this force equilibrium yielded a minimal overshoot on the order of 10^{-15}, which was extremely diverse from the experimental result because the hover model might not include dynamic and nonlinear traits in the actual yield.

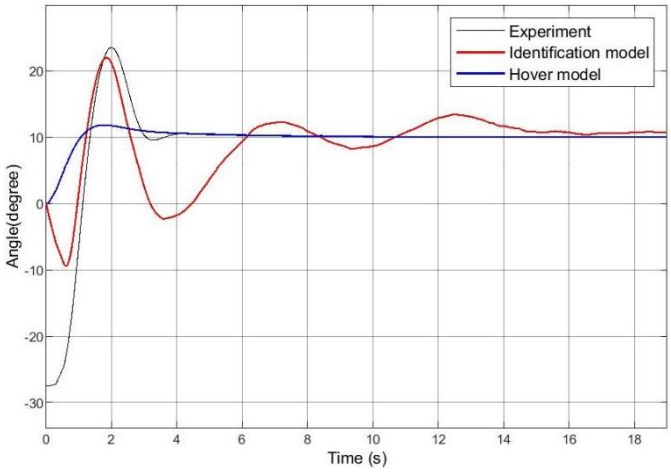

Figure 7. Comparison of roll angle between models and experiment

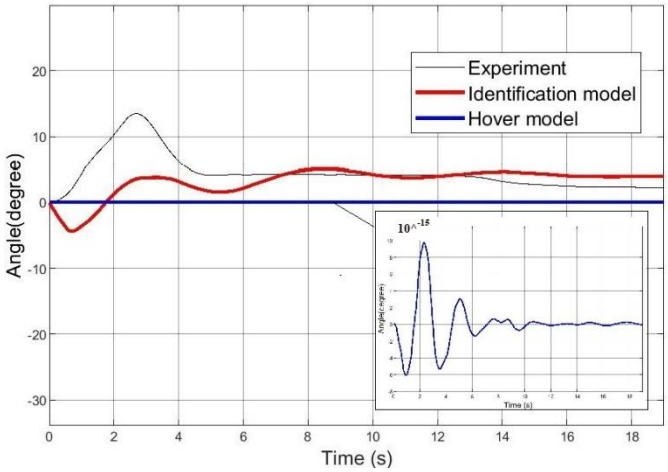

Figure 8. Comparison of pitch angle between models and experiment

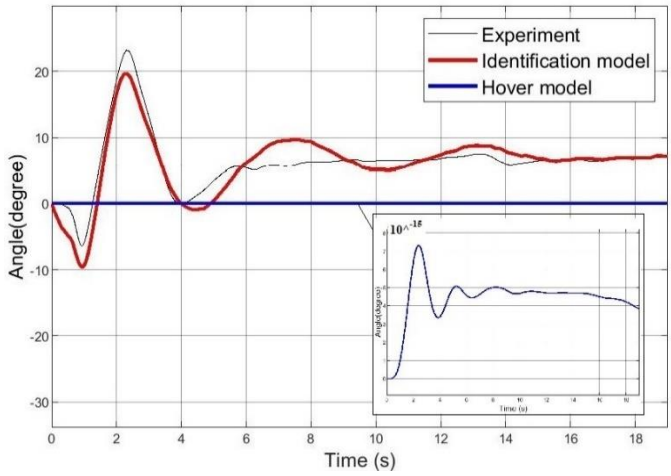

Figure 9. Comparison of yaw angle between models and experiment

A fascinating case happened at the yaw angle in Figure 9 that the identification method provided an accurate signal of both overshoot and error for validating the experimental results. Although the identification model and experimental overshoot results had slightly different results, namely 20° and 23°, respectively, they both had the same error result, around 7°. Again, the hover formula design signal gave a perfect value with overshoot and error approaching zero. The numerical results of the differences between the two models against the experiment are shown in Table II.

TABEL II. NUMERICAL RESULTS

Set angle	Overshoot		Error	
	Hover model (°)	**Identification model** (°)	**Hover model** (°)	**Identification model** (°)
Roll	11	1	0	1
Pitch	13	8	2	1
Yaw	23	3	7	0

The identification model achieved the better values of overshoot comparing with experimental by 1°, 3°, and 8° than hover model in all set angles. On the other hand, hover model only got more accurate in roll angle by 0° of difference, while pitch and yaw experienced better yields for identification way by 1° and 0°, respectively. However, the results of this hover model were much separate from the validation of the experimental results because the possibility of uncertainty, nonlinearity, and dynamic behavior was not inserted in the model. Due to better accuracy, the identification model of bicopter could be implemented in [10], [30] for its improvement.

IV. CONCLUSION

MIMO models of complex bicopter flight controls have been successfully constructed using hover principle and system identification methods. Comparing both techniques with validation of experimental results proves that the identification model was better than the hover model, especially the accuracy related to overshoot and error. Although the identification technique was quite troublesome because it firstly required input and output data from the system, it had better model accuracy. The experimental results comparison indicated that the identification model has the most accurate numerical yields for overshoot by 1°, 3°, and 8° in roll, pitch, and yaw angles. In addition, it achieved the excellent result of error differences by 1° and 0° for pitch and yaw angles, when the better value of error difference at roll angle occurred in the hover model by 0°. Therefore, the identification method was recommended to be used in control MIMO modelling in bicopter of UAV plants, especially optimization. Modelling based on the law of force balance on hover circumstances should be improved due to dynamic, uncertainty, and nonlinear conditions in the real experiment for future study.

REFERENCES

[1] R. M. Ariefianto, R. A. Aprilianto, H. Suryoatmojo, and S. Suwito, "Design and Implementation of Z-Source Inverter by Simple Boost Control Technique for Laboratory Scale Micro-Hydro Power Plant Application," *J. Tek. Elektro*, vol. 13, no. 2, pp. 62–70, 2021.

[2] F. Mohammadi et al., "Robust control strategies for microgrids: A review," IEEE Syst. J., vol. 16, no. 2, pp. 2401–2412, 2022, doi: 10.1109/JSYST.2021.3077213.

[3] A. Amini et al., "Learning robust control policies for end-to-end autonomous driving from data-driven simulation," IEEE Robot. Autom. Lett., vol. 5, no. 2, pp. 1143–1150, 2020.

[4] X. Yang and X. Zheng, "Adaptive nn backstepping control design for a 3-dof helicopter: Theory and experiments," *IEEE Trans. Ind. Electron.*, vol. 67, no. 5, pp. 3967–3979, 2019.

[5] M. Benosman, "Model-based vs data-driven adaptive control: an overview," Int. J. Adapt. Control Signal Process., vol. 32, no. 5, pp. 753–

776, 2018.
[6] L. Liu, S. Tian, D. Xue, T. Zhang, Y. Chen, and S. Zhang, "A review of industrial MIMO decoupling control," Int. J. Control. Autom. Syst., vol. 17, no. 5, pp. 1246–1254, 2019.
[7] Y. Yuan, D. Thomson, and R. Chen, "Propeller control strategy for coaxial compound helicopters," Proc. Inst. Mech. Eng. Part G J. Aerosp. Eng., vol. 233, no. 10, pp. 3775–3789, 2019.
[8] E. Apriaskar, F. Fahmizal, N. A. Salim, and D. Prastiyanto, "Performance Evaluation of Balancing Bicopter using P, PI, and PID Controller," *J. Tek. Elektro*, vol. 11, no. 2, pp. 44–49, 2019.
[9] Q. Zhang, Z. Liu, J. Zhao, and S. Zhang, "Modeling and attitude control of Bi-copter," in *2016 IEEE International Conference on Aircraft Utility Systems (AUS)*, 2016, pp. 172–176.
[10] J. A. Prakosa, E. Kurniawan, H. Adinanta, S. Suryadi, and M. I. Afandi, "Kajian Eksperimen Teknik Kontrol Penerbangan Posisi Tinggal Landas Drone Bikopter dengan Metode PID," *J. Otomasi Kontrol dan Instrumentasi*, vol. 12, no. 2, pp. 1–8, 2020, doi: 10.5614/joki.2020.12.2.1.
[11] D. Gesbert, M. Kountouris, R. W. Heath, C.-B. Chae, and T. Salzer, "Shifting the MIMO paradigm," *IEEE Signal Process. Mag.*, vol. 24, no. 5, pp. 36–46, 2007.
[12] K. Kudelina, T. Vaimann, A. Rassõlkin, and A. Kallaste, "Impact of Bearing Faults on Vibration Level of BLDC Motor," in IECON 2021--47th Annual Conference of the IEEE Industrial Electronics Society, 2021, pp. 1–6.
[13] S. Enache, A. Campeanu, V. Ion, and M.-A. Enache, "Aspects Regarding Tests of Three-Phase Asynchronous Motors with Single-Phase Supply," in *2019 16th Conference on Electrical Machines, Drives and Power Systems (ELMA)*, 2019, pp. 1–6.
[14] I. N. Ikhsan and S. A. Akbar, "Aplikasi Machine Vision pada Hexacopter untuk Deteksi Survival Kits di Bidang Mitigasi Bencana," *J. Tek. Elektro*, vol. 12, no. 2, pp. 72–79, 2020.
[15] X. He and Y. Wang, "Design and Trajectory Tracking Control of a New Bi-Copter UAV," IEEE Robot. Autom. Lett., vol. 7, no. 4, pp. 9191–9198, 2022.
[16] N. Nithyavathy, S. A. Kumar, D. Rahul, B. S. Kumar, E. R. Shanthini, and C. Naveen, "Detection of fire prone environment using Thermal Sensing Drone," in *IOP Conference Series: Materials Science and Engineering*, 2021, vol. 1055, no. 1, pp. 12006-12015.
[17] K. Fathoni, A. P. Pratama, N. A. Salim, and V. N. Sulistyawan, "Implementasi Kendali Keseimbangan Gerak Two Wheels Self Balancing Robot Menggunakan Fuzzy Logic," *J. Tek. Elektro*, vol. 13, no. 2, pp. 89–97, 2021.
[18] S. T. Muntaha, S. A. Hassan, H. Jung, and M. S. Hossain, "Energy efficiency and hover time optimization in UAV-based HetNets," *IEEE Trans. Intell. Transp. Syst.*, vol. 22, no. 8, pp. 5103–5111, 2021, doi: 10.1109/TITS.2020.3015256.
[19] J. A. Prakosa, E. Kurniawan, H. Adinanta, S. Suryadi, and P. Purwowibowo, "Experimental Based Identification Model of Low Fluid Flow Rate Control Systems," in *2020 International Conference on Radar, Antenna, Microwave, Electronics, and Telecommunications (ICRAMET)*, 2020, pp. 200–205.
[20] U. M. Guzey, E. H. Copur, S. Ozcan, A. C. Arican, B. M. Kocagil, and M. U. Salamci, "Experiment of sliding mode control with nonlinear sliding surface design for a 3-DOF helicopter model," in 2019 XXVII International Conference on Information, Communication and Automation Technologies (ICAT), 2019, pp. 1–6.
[21] H. Miranda, P. Cortés, J. I. Yuz, and J. Rodr\'\iguez, "Predictive torque control of induction machines based on state-space models," *IEEE Trans. Ind. Electron.*, vol. 56, no. 6, pp. 1916–1924, 2009.
[22] A. A. Ozdemir and S. Gumussoy, "Transfer function estimation in system identification toolbox via vector fitting," *IFAC-PapersOnLine*, vol. 50, no. 1, pp. 6232–6237, 2017.
[23] O. Loyola-Gonzalez, "Black-box vs. white-box: Understanding their advantages and weaknesses from a practical point of view," *IEEE Access*, vol. 7, pp. 154096–154113, 2019.
[24] J. A. Prakosa, S. Suryadi, E. Kurniawan, and H. Adinanta, "Kajian Identifikasi Model Eksperimen pada Kontrol Kecepatan Motor DC," *J. Otomasi Kontrol dan Instrumentasi*, vol. 13, no. 1, pp. 27–35, 2021, doi: 10.5614/joki.2021.13.1.3.
[25] C. H. B. Apribowo, H. Maghfiroh, and A. T. Laksita, "Design close-loop control of BLDC motor speed using PID method in solar power with matlab/simulink," in AIP Conference Proceedings, 2020, vol. 2217, no. 1, p. 30137.
[26] M. Jirgl, L. Obsilova, J. Boril, and R. Jalovecky, "Parameter identification for pilot behaviour model using the MATLAB system identification toolbox," in *2017 International Conference on Military Technologies (ICMT)*, 2017, pp. 582–587.
[27] D. Prastiyanto, E. Apriaskar, P. A. Handayani, R. Destanto, M. A. Malik, and A. E. Ramadhan, "Identification of microwave heating system with symmetrical octagonal tube cavity using ARX model," in *IOP Conference Series: Earth and Environmental Science*, 2022, vol. 969, no. 1, pp. 12025-12033.
[28] M. Arrofiq, E. Apriaskar, A. Mayub, and others, "Rigorous Modelling Steps on Roll Movement of Balancing Bicopter using Multi-level Periodic Perturbation Signals," in *2019 6th International Conference on Instrumentation, Control, and Automation (ICA)*, 2019, pp. 52–57.
[29] R. Szplet and D. Szymanowski Rafałand Sondej, "Measurement uncertainty of precise interpolating time counters," IEEE Trans. Instrum. Meas., vol. 68, no. 11, pp. 4348–4356, 2019.
[30] M. Nkemdirim, S. Dharan, H. Chaoui, and S. Miah, "LQR control of a 3-DOF helicopter system," *Int. J. Dyn. Control*, vol. 10, no. 4, pp. 1084–1093, 2022.

APPENDIX

Experimental Setup

A bicopter simulator plant, scilicet 3 DOF helicopters in Figure 4, can be run by arranging the main components in Figure 10. In this bicopter plant, two motors are driven by a power connected to the amplifier. The PC can control both motors on the bicopter simulator via an amplifier connected through its USB cable. Angle sensors such as roll, yaw, and pitch are embedded in the 3 DOF helicopter tool to measure the feedback signal from the angular position of the bicopter simulator. The components must be connected via cables that build a closed-loop system, as shown in Figure 11.

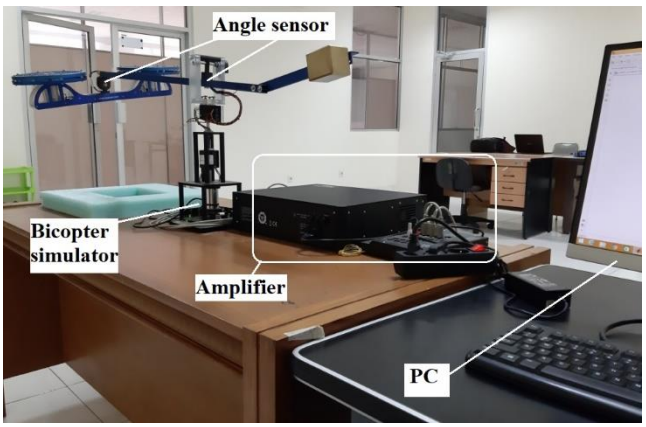

Figure 10. Hardware of bicopter simulator setup

A bicopter simulator plant, scilicet 3 DOF helicopters in Figure 4, can be run by arranging the main components in Figure 10. In this bicopter plant, two motors are driven by a power connected to the amplifier. The PC can control both motors on the bicopter simulator via an amplifier connected through its USB cable. Angle sensors such as roll, yaw, and pitch are embedded in the 3 DOF helicopter tool to measure the feedback signal from the angular position of the bicopter simulator. The components must be connected via cables that build a closed-loop system, as shown in Figure 11.

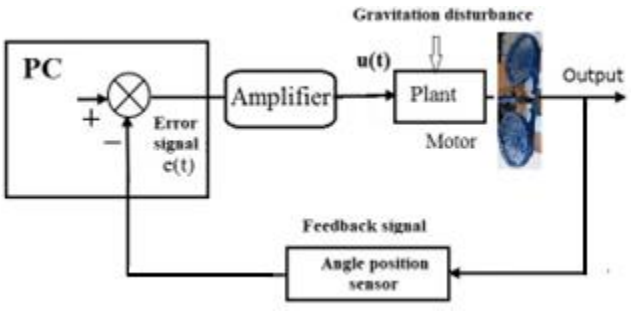

Figure 11. Close loop of bicopter simulator system

The close loop system at the 3 DOF helicopter facility employs Matlab and Simulink software in Figure 12 to operate it. This software can compute and simulate all of the above equations. The proposed method can be designed by Matlab/Simulink, which can be validated experimentally utilizing this bicopter simulator platform. For example, this diagram is applied to set the desired angle of bicopter.

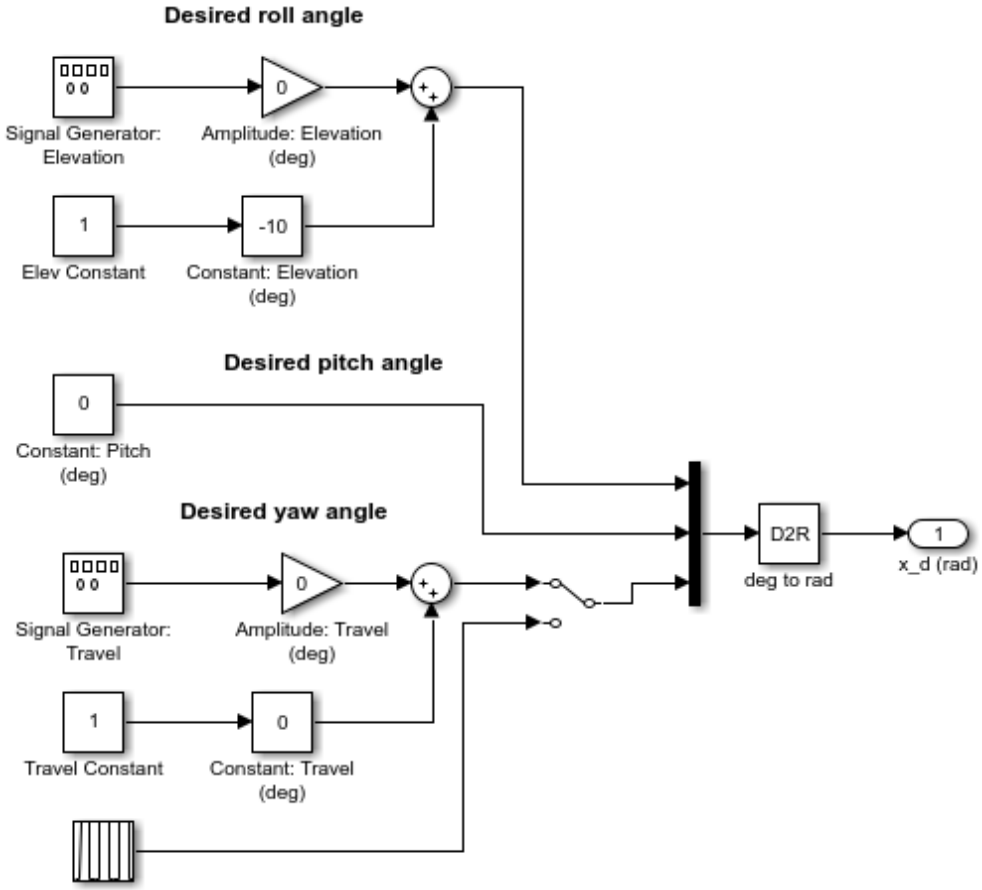

Figure 12. Software of bicopter simulator setup